Optimization of hydrogen storage capacity in silica-supported low valent Ti systems exploiting Kubas binding of hydrogen

Ahmad Hamaed [a,*], Tuan K.A. Hoang [a], Michel Trudeau [a b], David M. Antonelli [a]

[a] Department of Chemistry, University of Windsor, 401 Sunset Avenue, Windsor, Ontario, Canada N9B 3P4
[b] Chemistry and Materials, Hydro-Québec Research Institute, Varennes, Quebec, Canada J3X 1S1

ABSTRACT

Silica-based materials grafted with low valent Ti fragments for Kubas-type binding of hydrogen were optimized for hydrogen adsorption capacity by varying the surface area, pore size, loading levels, and type of organometallic precursor. All materials were characterized by XRD, nitrogen adsorption, and XPS where appropriate. The surface area of HMS silica was optimized by varying silica-to-surfactant molar ratio, and also by tuning the pore size by varying the surfactant's carbon chain length (C_6, C_8, C_{10}, C_{12}). Then Ti fragments originating from either benzyl, allyl, or methyl Ti precursors were grafted onto the optimal HMS surface at different loading levels to arrive at Ti grafted HMS materials with H_2 storage capacities and binding properties superior to those previously reported by our group for benzyl Ti (III) species on silica. HMS prepared with dodecylamine using a silica:surfactant ratio of 3:1 and subsequently grafted with 0.2 M equiv. of $TiBz_4$ had the highest H_2 adsorption at 2.45 wt% at 77 k and 60 atm, which equates to an average of 3.98 H_2 molecule per Ti metal center, just one H_2 molecule short of the theoretical saturation limit of 5 H_2/Ti predicted by the 18-electron rule. The H_2 adsorption capacities of Me_3Ti-HMS and $Allyl_3Ti$-HMS prepared using the same optimized sample of C_{12}-HMS silica at a 3:1 Si:surfactant ratio possessed H_2 adsorption values corresponding to 2.4 and 2.27 H_2 per Ti center, respectively, at 60 atm and 77 K. This performance level is significantly lower than that of the benzyl Ti (III) system. The binding enthalpies of the benzyl Ti (III) material increase with H_2 coverage to 23 kJ/mol, while the enthalpies for the newly synthesized Me_3Ti-HMS and $Allyl_3Ti$-HMS materials increase with H_2 coverage to a maximum of 2.66 and 4.17 kJ/mol, respectively. XPS studies on these materials suggested a trend in π-back donating ability on the Ti (III) centers of methyl > allyl > benzyl, opposite that observed experimentally. The reason for the diminished performance of the allyl and methyl Ti (III) systems may thus be related to the presence of THF ligands blocking coordination sites in the allyl and methyl systems. THF is not present in the benzyl system because this solvent is not required for synthesis.

© 2009 Elsevier B.V. All rights reserved.

1. Introduction

Research into hydrogen storage has become increasingly important due to the increased demands placed on world oil reserves as well as the various environmental issues related to global warming and the consumption of fossil fuels [1]. Hydrogen is an ideal fuel because it has the highest energy per gram of any substance and only emits water as a combustion product, therefore avoiding green house gas emissions. The DOE has set system targets of 9.0 wt% and 81 kg/m³ for 2015 [2], and while some materials meet or surpass one of these values, there is no material that is close to meeting both of them. In addition to this, there are many often overlooked factors such as kinetics or release, thermal conductivity, and binding enthalpy that must be considered before a hydro-

gen storage material can become practical. Isoteric heats of adsorption are of special importance because they govern the strength of binding of the hydrogen to the chemical carrier and also determine the amount of heat released or required on charge/discharge, respectively. Materials such as hydrides, which possess enthalpies of 70 kJ/mol and higher, release enormous amounts of heat on filling and require equally large amounts of heat to liberate the hydrogen when it is required as fuel. This creates problems with heat management and also drastically lowers the effective energy storage capacity of the system. Poor reversibility and slow kinetics are also problems with many metal hydride [3] systems including MgH_2, $NaAlH_4$, and NH_3BH_3. As an alternative to hydrides, materials such as MOFs [4–6] and porous carbons [7–9] absorb hydrogen on their vast internal network of surface area, and offer great kinetic advantages over hydrides. However, their low binding enthalpies of generally less than 10 kJ/mol, while facilitating heat management on refueling, necessitate cooling to 77 K for optimal performance, again diminishing the energy

storage capacity of the system. For these reason, it has been proposed that materials possessing 20–30 kJ/mol binding enthalpies may be ideal for on board hydrogen storage applications [10,11]. These moderate isoteric heats of adsorption do not cause as much difficulty in terms of heat management, but provide enough thermal stability to the interaction between the hydrogen and the material to perform at temperatures higher than 77 K. The Kubas interaction [12,13], effectively a σ–π ligand interaction between a hydrogen molecule and a metal center, affords these ideal enthalpies in conjunction with predicted high storage capacities in many hypothetical systems, most involving early transition metals [9–11]. There is also strong evidence for such an interaction at apical metal centers in many MOF and Prussian Blue [14] framework materials. In 2008 we reported the first example of a material that possessed an enthalpy in the target 20–30 kJ/mol range [15]. This system was comprised of Ti (III) benzyl units on mesoporous silica which increased the performance of the system from 1.2 wt% to 1.65 wt% at 77 K. The tailored Ti fragments held 3 H_2 per unit under these conditions while also retaining 41% of their capacity at room temperature. These materials constituted a substantial leap forward by demonstrating that Kubas binding may represent a potential answer to many hydrogen storage problems. In this paper we optimize the performance of this Ti (III) system by adjusting several synthetic parameters and exploring other Ti precursors. We show that after fine tuning of the surface area, pore size, and synthetic protocol that HMS silica grafted with 0.2 equiv. of $TiBz_4$ reaches 2.45 wt% adsorption at 77 k and 60 atm after activation to the Ti (III) form, which equates to 3.98 H_2 on average per Ti center. This is close to the theoretical maximum of 5 H_2 per Ti predicted by the 18-electron rule and demonstrates that organometallic fragments can carry more hydrogen ligands per metal at high pressure and low temperature than the maximum observed in an isolated organometallic compound at room temperature and pressure.

2. Results and discussion

2.1. Variation of silica-to-surfactant molar ratio

Since hydrogen adsorption in Ti grafted mesoporous silicas contains a large component of physisorption due to the huge internal surface area, we maximized the surface area of the hexagonally-packed mesoporous silica by varying the silica-to-surfactant ratio (Table 1). The highest surface area of 1448 m^2/g was obtained when the Si to dodecylamine ratio was 4:1. Three other HMS silica
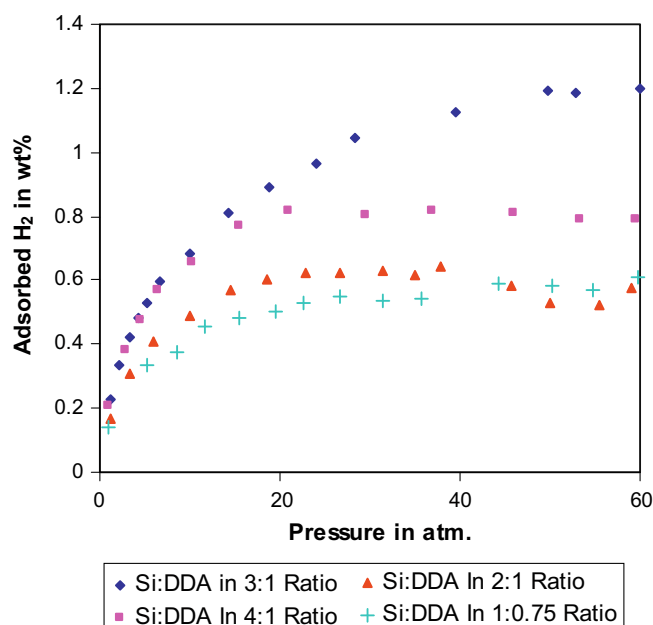

Fig. 1. Hydrogen adsorption isotherms at 77 K for mesoporous silica synthesized using different molar ratios of tetraethyl orthosilicate:dodecylamine.

samples were prepared with silica-to-surfactant ratios of 3:1, 2:1, and 1:0.75 and possessed BET surface areas of 1165, 1117, and 822 m^2/g, respectively. The surprising fact was that the hydrogen adsorption capacity (excess storage) of the 4:1 sample of HMS at 77 K was lower (0.75 wt%, and a surface area of 1448 m^2/g) than that prepared with a Si:DDA ratio of 3:1 (1.2 wt% and a surface area of 1165 m^2/g). The higher adsorption capacity of the 3:1 silica may be due to differences in micropore volume of the two samples, which may beyond the accuracy of nitrogen adsorption measurement. The 2:1, and 1:0.75 samples possessed H_2 adsorption values of 0.75 and 0.90 wt%, respectively, at 77 K, lower than that prepared with 3:1 ratio (Fig. 1). The skeletal densities of the silicas ranged from 1.62 to 2.33 g/cc. The total storage was also measured from the apparent densities shown in Table 1. This is a measurement of the total hydrogen present on the surface and as compressed gas in the pores in a given volume of material normalized to the sample weight. This number is highly dependent on the compression of the sample, but is the only way of determining how much hydrogen is present in a sample of a porous solid under pressure. Again, the material synthesized at a Si:DDA ratio of 3:1 showed the highest performance, with a total gravimetric storage of 19.06 wt%.

2.2. Variation of pore size

Since microporous materials are believed to absorb more hydrogen due to capillary action, HMS silica with smaller pore sizes were synthesized by shortening the surfactant chain length. The hexylamine, octylamine, decylamine, and dodecylamine templates, possessing 6, 8, 10, and 12-carbon chain lengths were thus independently employed in the synthesis procedure of HMS. The corresponding template free materials had BJH pore sizes of 12, 18, 22, and 25 Å, respectively. The pristine C_6-HMS and C_8-HMS silicas had higher hydrogen adsorption capacity (1.38 and 1.60 wt%, respectively) than that synthesized by using the dodecylamine template (1.20 wt%) (Table 2, and Fig. 2). But after grafting the surface of the C_6-HMS or C_8-HMS with tetrabenzyl titanium at a 0.2 M equiv. loading level, the adsorption capacities of these silicas decreased dramatically, from 1.38 to 0.70 wt% and from 1.6 to 0.95,

Table 1
A summary of the apparent density, skeletal density, gravimetric storage, gravimetric adsorption, and surface area of all HMS pristine synthesized using different molar ratios of tetraethyl orthosilicate to dodecylamine.

Sample	Apparent density (g/ml)	Skeletal density (g/ml)	Gravity storage at 100 atm (wt%)	Gravity adsorption at saturation (wt%)	Surface area (m^2/g)
C_{12}-HMS Si:DDA 4:1	0.18	2.33	17.82	0.75	1448
C_{12}-HMS Si:DDA 3:1	0.17	2.13	19.06	1.20	1165
C_{12}-HMS Si:DDA 2:1	0.19	2.04	16.10	0.75	1117
C_{12}-HMS Si:DDA 1:0.75	0.17	2.16	18.10	0.90	922

Table 2
Hydrogen sorption capacity of micro- and mesoporous silica at 77 K with different surface areas and pore sizes synthesized using amine templating agents of various chain lengths.

Sample	Apparent density (g/ml)	Skeletal density (g/ml)	Pore size (Å)	Gravity storage at 100 atm (wt%)	Gravity adsorption at saturation (wt%)	Surface area in (m²/g)
C_6-HMS	0.15	1.92	12	21.15	1.38	1074
C_8-HMS	0.19	1.61	18	17.18	1.60	1321
C_{10}-HMS	0.14	1.52	22	20.61	1.01	1206
C_{12}-HMS	0.168	2.13	25	19.06	1.20	1165

not the case with the C_{12} material where the H_2 adsorption increases from 1.20 wt% for the pristine to 2.45 wt% after grafting with 0.2 M equiv. of TiBz$_4$. This value of 2.45 wt% is much higher than the 1.6 wt% previously reported for tetrabenzyl titanium grafted to C_{12}-HMS, likely because of the higher surface area of the sample employed in this study leading to a greater number of silanol anchoring points for the Ti fragments in the material. The smaller pores of the C_6 and C_8-HMS yield materials of higher surface areas which allows a larger quantity of hydrogen gas to physisorb on the surface, but at the same time the pore size of these microporous silicas are too small to allow the unencumbered incorporation of the large tetrabenzyl Ti fragments onto the surface, thus restricting the Ti loading level and/or effectiveness of the Ti centers for hydrogen binding. This finding is consistent with a previous study in our group, which explored the H_2 storage of microporous and mesoporous titanium oxide treated with bis (toluene) Ti [16,17]. C_{10}-Ti-TMS1 was found to have an adsorption capacity of 1.01 wt%, lower than that of C_{12}-Ti-TMS1, even though it had a higher surface area (see Fig. 3).

From the above experiments, it appears that the C_{12}-HMS prepared by using silica-to-surfactant ratio of 3:1 is the best support for hydrogen storage in this study. In all subsequent experiments this same sample of silica was grafted with various Ti fragments at different loading levels, in order to optimize the hydrogen adsorption capacity of these materials.

2.3. Variation of metal-fragment precursor and precursor loading levels

By grafting the surface of C_{12}-HMS, prepared from a 3:1 molar ratio of TEOS and dodecylamine, with 0.2 equiv. of tetrabenzyl titanium we reached 2.45 wt% adsorption, which equates to an average of 3.98 H_2 molecules per Ti metal center, only one H_2 molecule short of the saturation level predicted by the 18-electron rule. This is the highest adsorption value reached so far for mesoporous metal oxides (Table 3). The room temperature adsorption of this material was 0.76 wt%, indicating that 31% of the H_2 was retained per Ti at 25 °C. This equates to 1.23 Ti per metal center, on the basis of 4.08 wt% Ti in the sample. This compares to 0.44 wt% adsorption in pure mesoporous silica under these conditions. Materials prepared at lower or higher ratios yielded lower hydrogen adsorption results. It appears that the material prepared with 0.1 equiv. of Ti does not possess enough Ti units per square nanometer to maximize the hydrogen storage performance, while samples prepared with higher levels of Ti than 0.2 equiv., have lower performance due to clustering on the surface.

When tribenzyl titanium is anchored onto the surface of C_{12}-HMS silica, the adsorption capacities are slightly lower than those of their tetrabenzyl Ti counterparts (i.e., 2.04 wt% for the 0.2TiBz$_3$-HMS, compared to 2.45 wt% for that of 0.2TiBz$_4$-HMS) (Table 4, and Fig. 4). This may be due to metal clustering of low valent Ti on the
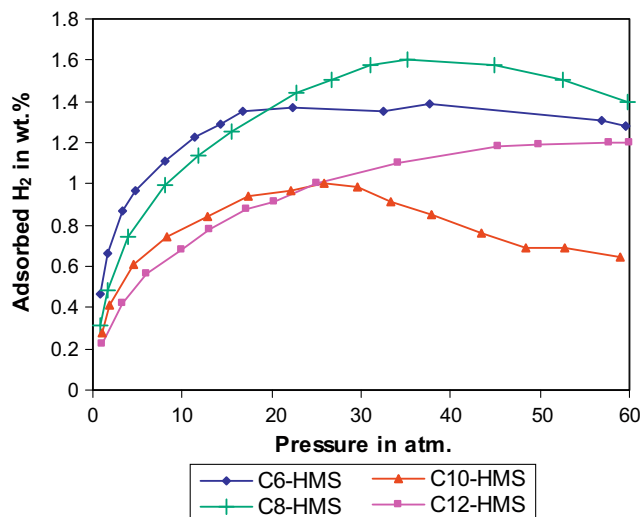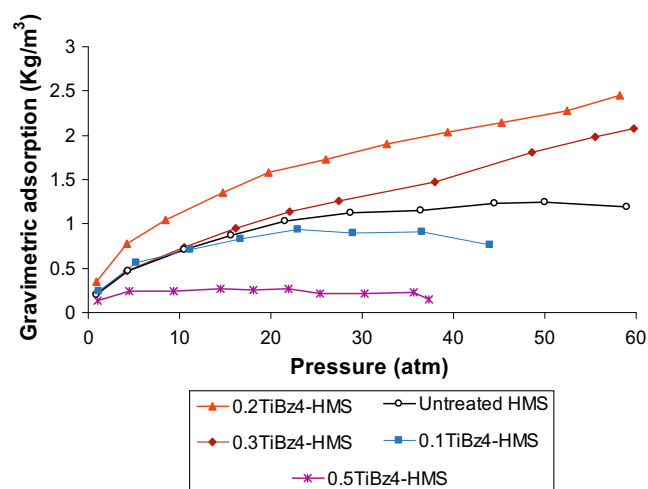

Fig. 3. Hydrogen adsorption isotherms at 77 K of C_{12}-HMS grafted with various molar equivalents of tetrabenzyl Ti.

Table 3
Summarizing the storage and adsorption capacities of C_{12}-HMS treated with different molar equivalents of tetrabenzyl Ti.

Sample	Apparent density (g/cc)	Skeletal density (g/cc)	Gravity storage (wt%)	Gravity adsorption (wt%)
0.1TiBz$_4$-C_{12}-HMS	0.17	1.96	17.68	0.95
0.2TiBz$_4$-C_{12}-HMS	0.16	1.62	21.45	2.45
0.3TiBz$_4$-C_{12}-HMS	0.17	1.99	19.67	2.04
0.5TiBz$_4$-C_{12}-HMS	0.20	1.86	13.04	0.26

Fig. 2. Hydrogen adsorption isotherms at 77 K of C_6, C_8, C_{10} and C_{12}-HMS.

Table 4
Summarizing the storage and adsorption capacities of C_{12}-HMS treated with different molar equivalents of tribenzyl Ti.

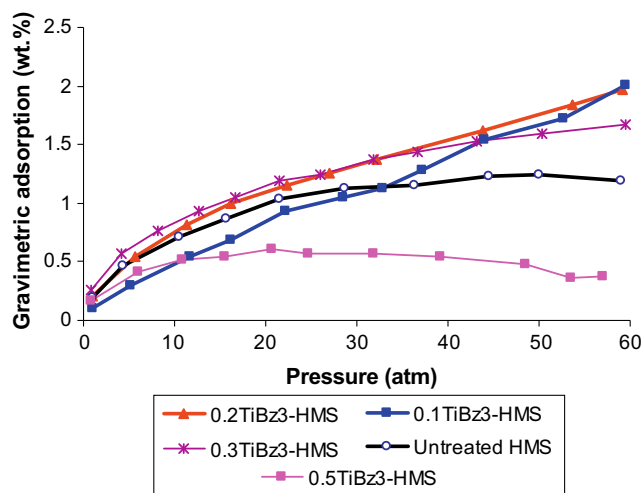| Sample	Apparent density (g/cc)	Skeletal density (g/cc)	Gravity storage (wt%)	Gravity adsorption (wt%)
0.1TiBz$_3$-C$_{12}$-HMS	0.16	0.94	19.26	1.99
0.2TiBz$_3$-C$_{12}$-HMS	0.17	0.93	17.48	2.02
0.3TiBz$_3$-C$_{12}$-HMS	0.31	1.31	10.03	1.74
0.5TiBz$_3$-C$_{12}$-HMS	0.34	1.38	7.35	0.62

Fig. 4. Hydrogen adsorption isotherms at 77 K of C_{12}-HMS grafted with various molar equivalents of (benzyl)$_3$Ti.

surface, which disfavors H_2 binding. The Ti (III) fragments are more reactive than the Ti (IV) fragments and clustering of Ti (III) units by the creation of Ti–Ti bonds may compete with the anchoring to surface hydroxyl groups, making Ti (IV) deposition, followed by thermal cleavage of the benzyl–Ti bond yield the active Ti (III) species, more selective and effective than Ti (III) deposition.

Finally, commercially available 380-Aerosil hydrophilic fumed silica with a surface area of 380 m^2/g obtained from Evonic-Degussa Chemicals, was tested for hydrogen adsorption capacity before and after grafting with tetrabenzyl Ti. The pristine Aerosil has an adsorption capacity of 1.25 wt% at 77 K and 60 atm, similar to that of C_{12}-HMS (1.2 wt%). When grafted with 0.2 M equiv. of TiBz$_4$ this material shows an adsorption of only 1.15 wt%. An almost identical adsorption capacity was obtained when this material was coated with 0.3 equiv. of TiBz$_4$. When grafted with 0.5 equiv. of TiBz$_4$ the adsorption capacity increased to 1.40 wt%. Beyond this loading level the adsorption capacity begins to decrease to levels below that of the untreated sample. The reason for this may be due to different surface diffusion properties and concentration of surface anchoring sites in the corresponding silicas effecting the surface anchoring process. The silanol group density of 380-Aerosil was approximated to an average of 1.25 SiOH/nm^2 as measured by the LiAlH$_4$ method [18], compared to 4.6 SiOH/nm^2 for that of HMS [19] (see Table 5).

2.4. Ti(CH$_3$)$_3$ grafted on HMS

Since different ligands in the Ti (III) coordination sphere are likely to influence hydrogen binding either electronically, through

Table 5
Summarizing the adsorption capacities of plain and treated 380-Aerosil with different molar ratios of tetrabenzyl Ti.

Sample	Skeletal density (g/cc)	Gravity adsorption (wt%)
Plain 380-Aerosil (compressed)	1.79	1.25
0.2TiBz4-380-Aerosil	1.58	1.15
0.3TiBz4-380-Aerosil	1.48	1.15
0.5TiBz4-380-Aerosil	1.39	1.40

their ability to donate electrons to the Ti center and thus strengthen π-back bonding to the H–H antibonding orbital, or sterically, by influencing the ease in which H_2 can access the open coordination sites on Ti, it is likely that different Ti (III) precursors will lead to grafted mesoporous silicas with different hydrogen adsorption properties. The benzyl ligand is electron withdrawing, can adopt an η^3 coordination mode thereby shutting down a coordination site, and is somewhat heavy, all factors may lead to diminished hydrogen storage performance in this system. In previous unpublished studies we attempted to remove the benzyl ligand by hydrogenation according to a literature report on benzyl Ti grafted silicas for Ziegler-Natta catalysis [20] to leave behind a Ti (III) hydride, however the resulting material possessed a hydrogen adsorption capacity almost identical to that of the material before hydrogenation. The reason for this is not known, as a hydride ligand should provide a more facile steric environment for hydrogen binding and contributes less weight than a benzyl ligand. In order to explore the effects of different ligands and precursors, we prepared a sample of HMS silica grafted with TiMe$_3$. This compound is thermally unstable and can only be synthesized in THF solution at $-78\,°C$. It exists as a THF adduct in solution, and decomposes to form methane and various carbenoid species at ambient temperature. The experimental results (Table 6, and Fig. 5) showed that the adsorption capacity of TiMe$_3$-HMS prepared at 0.2, 0.3 and 0.5 equiv. loading levels is actually lower than that of the benzyl grafted materials (1.48, 1.44, and 1.47 wt%, respectively). This may due to the influence of coordinated THF on the Ti center, which blocks coordination sites, creates steric bulk around the Ti center, and increases the weight of the system, while also withdrawing electron density through the coordinated oxygen atom. Scheme 1 shows a depiction of the possible H_2 binding geometries of TiMe$_3$ grafted HMS on the silica surface. Decomposition of this species on the surface to methane and carbenoid species, less able to bind H_2, may also be occurring. There is also the possibility that the η^3 coordination of the benzyl ligand is required to protect the naked low-coordinate Ti (III) center from decomposition pathways and that this ligand only adopts an η^1 coordination in the presence of excess H_2, which can occupy the vacated orbital as an L-type ligand. In order to test this hypothesis, tris-allyl Ti grafted HMS was also prepared. The allyl ligand can also adopt η^1 or η^3 configura-

Table 6
Summarizing the adsorption capacities of C_{12}-HMS treated with different molar equivalents of TiMe$_3$.

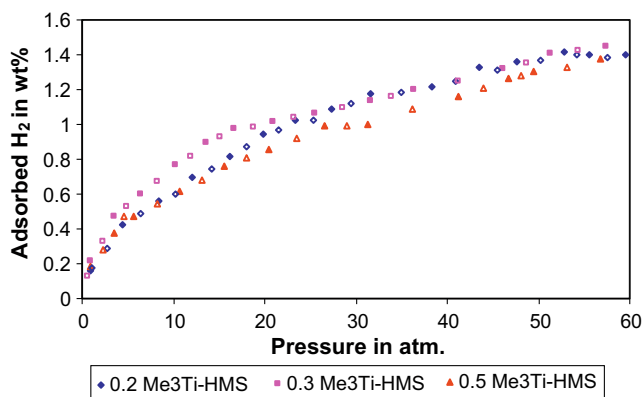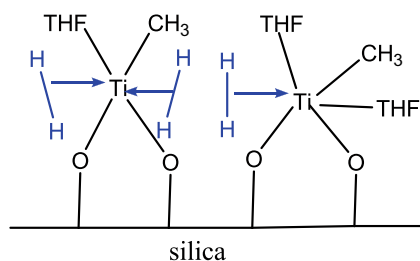| Sample	Apparent density (g/cc)	Skeletal density (g/cc)	Gravity storage (wt%)	Gravity adsorption (wt%)
0.2TiMe$_3$-C$_{12}$-HMS	0.18	1.55	17.84	1.48
0.3TiMe$_3$-C$_{12}$-HMS	0.18	1.49	17.11	1.44
0.5TiMe$_3$-C$_{12}$-HMS	0.30	1.73	11.04	1.47

Fig. 5. Excess hydrogen adsorption (filled symbols) and desorption (unfilled symbols) isotherms at 77 K and 60 atm of HMS treated with 0.2, 0.3, and 0.5 M equiv. of TiMe$_3$.

Scheme 1. Material prepared by coating HMS surface with trimethyl Ti precursor.

tions and may provide a stabilizing effect, if this is indeed necessary, and is also lighter and less bulky than the benzyl ligand, both factors which should lead to improved hydrogen storage performance.

2.5. Ti(Allyl)$_3$ grafted on HMS

Ti(Allyl)$_3$ grafted HMS silica was prepared at loading levels of 0.2, 0.3, and 0.5 equiv. The results are summarized in Fig. 6 and Table 7. The hydrogen adsorption results were even lower than those
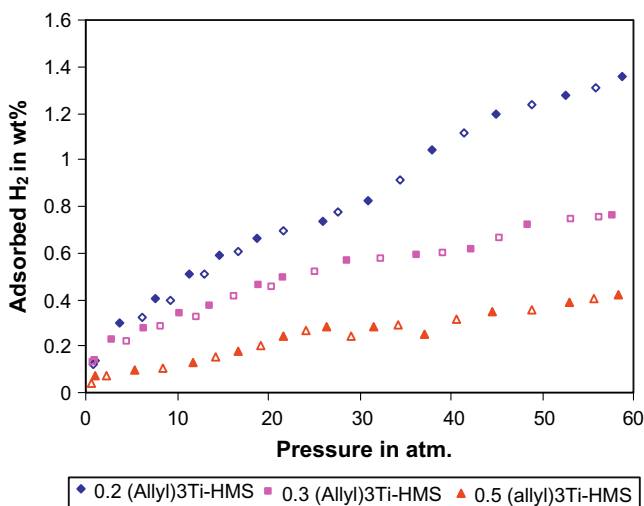

Fig. 6. Excess hydrogen adsorption (filled symbols) and desorption (unfilled symbols) isotherms at 77 K and 60 atm of HMS treated with 0.2, 0.3, and 0.5 M equiv. of (Allyl)$_3$Ti.

Table 7
Summarizing the adsorption capacities of C$_{12}$-HMS treated with different molar ratios of triallyl Ti.

Sample	Apparent density (g/cc)	Skeletal density (g/cc)	Gravity storage (wt%)	Gravity adsorption (wt%)
0.2Ti(Allyl)$_3$-C$_{12}$-HMS	0.33	1.67	9.36	1.40
0.3Ti(Allyl)$_3$-C$_{12}$-HMS	0.28	1.70	10.66	0.72
0.5Ti(Allyl)$_3$-C$_{12}$-HMS	0.35	1.50	5.28	0.51

in the trimethyl case (1.40, 0.72, and 0.51 wt%, respectively). Also, while the TiMe$_3$ system showed little variation between the different loading levels in performance, the corresponding allyl system showed a precipitous drop off on increasing the loading to 0.3 from 0.2. This suggests that clustering may be occurring on the silica surface, essentially shutting down a large proportion of the hydrogen binding to the metal center. This demonstrates that the allyl ligand is much less efficient than the benzyl ligand in preventing surface clustering, either because of its lower steric profile, or because it is less able to adopt an η^3 binding mode due to the influence of coordinated THF, the presence of which further diminishes performance for reasons discussed above (see Scheme 2).

2.6. XPS studies and enthalpies

To investigate the nature of the surface species in the benzyl, methyl and allyl systems and gain further information on the trends in hydrogen adsorption performance, X-ray photoelectron spectroscopy (XPS) studies were conducted (Fig. 7). This is a very powerful method for revealing the electron density about a metal center and should thus reveal which system is electronically most disposed to π-back bonding to hydrogen. The spectra of the surfaces in the Ti 2p region demonstrate a trend in reduced binding energies in the Ti 2p$_{3/2}$ emission as you go from Me to allyl to benzyl, with binding energies at 458.5, 458.8, and 459.4 eV, respectively. All binding energies (BEs) were referenced to the C 1s hydrocarbon peak at 284.8 eV. In addition, the XPS spectrum of trimethyl Ti-HMS has a shoulder in the binding energy (BE) range of Ti(III) chemical state at 456.2 eV [21], suggesting that decomposition to a lower valent Ti species may have occured.

The binding enthalpies (Fig. 8) of these materials were calculated by a variant of the Clausius–Clapyron equation [22] from hydrogen adsorption data at 77 and 87 K. In all the cases, ΔH increases as H$_2$ capacity increases. Steep slopes were obtained for the cases of tris and tetra benzyl Ti-HMS, increasing to 23.53 and 22.15 kJ/mol, respectively. But, in the case of the (Methyl)$_3$Ti and
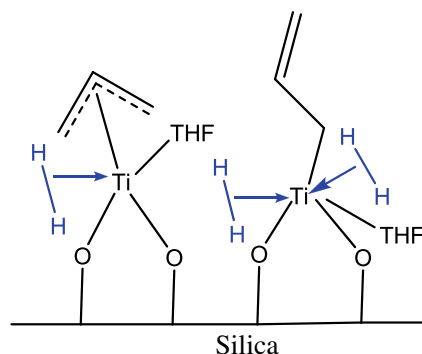
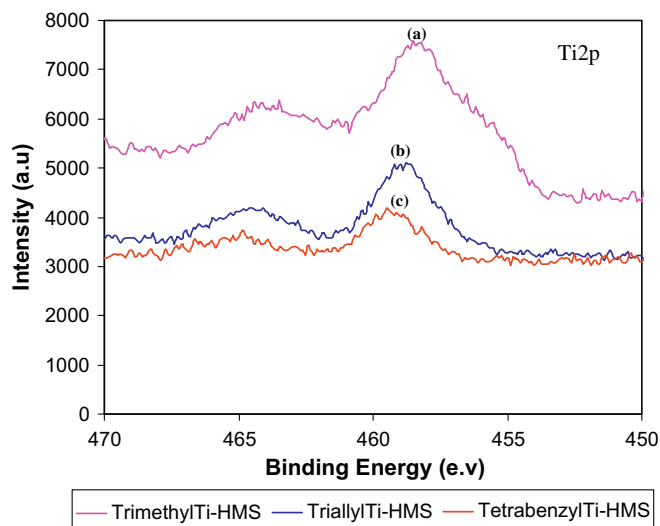**Scheme 2.** Material prepared by grafting the HMS surface with triallyl Ti precursor.

Fig. 7. Ti 2p XPS spectra of HMS treated with 0.2 equiv. of (a) trimethyl Ti, (b) triallyl Ti, and (c) tetrabenzyl Ti.
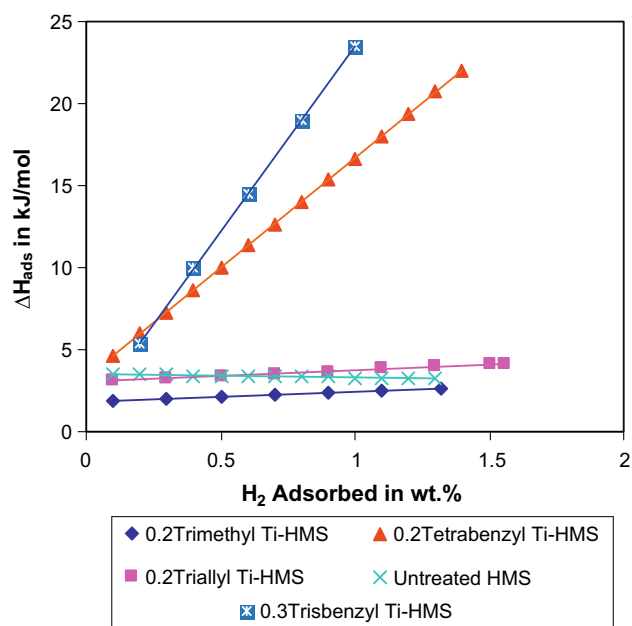

Fig. 8. Hydrogen binding enthalpies of pristine HMS ($\times$), 0.2Me$_3$Ti-HMS ($\blacklozenge$), 0.2(Allyl)$_3$Ti-HMS ($\blacksquare$), 0.2Bz$_4$Ti-HMS ($\blacktriangle$), and 0.3Bz$_3$Ti-HMS ( ).

(Allyl)$_3$Ti-HMS the binding enthalpies increase more slowly with H$_2$ adsorption, and reach maxima at only 2.66 and 4.17 kJ/mol, respectively. This observation is in keeping with the trend in hydrogen adsorption characteristics, the benzyl systems possessing both the higher enthalpies and the better storage performance. However, both the hydrogen adsorption properties and the enthalpies of these materials are surprising in light of the XPS data which suggests that the methyl is the most electron rich, followed by the allyl, and then the benzyl. If π-back bonding were the only contributing factor to improved performance, then the methyl should be the best, followed by the allyl, and then the benzyl. This clearly suggests that many other factors such as the coordination number and geometry as well as the steric environment about the metal fragment, are equally important in hydrogen storage performance in this system.

3. Conclusion

In summary, we have demonstrated that by varying the Si-to-template molar ratio, the carbon chain length of surfactant, the organometallic Ti-fragment precursor on the surface, and the loading level of that precursor, we can arrive at a material with 2.45 wt% hydrogen adsorption at 77 K and 60 atm, which compares to 1.2 wt% for untreated silica under the same conditions, and 1.6 wt% under these conditions for our best benzyl Ti grafted mesoporous silica studied previously. This 2.45 wt% demonstrates that the type of silica used as a support is very crucial to obtaining the highest performance, and corresponds to almost 4 H$_2$ per Ti, only one less than the theoretic limit of five predicted by the 18-electron rule. This is much higher than that observed previously for a poly-hapto Kubas compound and suggests that at lower temperatures and higher pressures certain metal centers can be forced to adopt up to 4 H$_2$ per metal. Smaller methyl and allyl ligands have no advantage over benzyl, contrary to what was expected on the basis of sterics, weight, and electronic properties. The enthalpies of the benzyl Ti system were in the predicted 20–30 kJ/mol range for room temperature performance, and as expected from the inferior hydrogen adsorption abilities, but the allyl and methyl systems had enthalpies of less than 5 kJ/mol. These data all suggest that it is difficult to predict on sterics and electron donating ability alone what the hydrogen storage capacity of metal grafted fragments on silica should be.

4. Experimental

All chemicals, unless otherwise stated, were obtained from Aldrich. H$_2$, CO$_2$ and N$_2$ gases were obtained from Praxair Canada Inc.

4.1. Synthesis of tetrabenzyl titanium [23]

To a solution of C$_6$H$_5$CH$_2$MgCl (100 ml, 1 M in diethyl ether) in diethyl ether (100 ml) at −15 °C was added a solution of TiCl$_4$ (2.5 ml, 22.8 mmol) in pentane (100 ml) dropwise over 2 h. The mixture was stirred for 3 h at −15 °C and filtered. The solid residue was washed with diethyl ether (2 × 50 ml) and the combined filtrate and washings were reduced *in vacuo*. The residue was dissolved in pentane (50 ml) and filtered, followed by further washing of the residue with pentane (2 × 50 ml). The filtrate and pentane washings were concentrated to approximately 70 ml and cooled to −30 °C overnight to yield a dark red-brown crystalline product.

4.2. Synthesis of tribenzyl titanium [24]

Tribenzyl titanium was obtained at 0 °C in a toluene solution by the reaction of tetrabenzyltatanium with ethyllithium for 2 h. The resulting benzyl lithium was precipitated by carboxylation with dry CO$_2$ at −78 °C. A tribenzyl titanium solution was obtained after filtration. Crystallization gave a 65% yield with respect to the initial quantity of tetrabenzyl titanium.

4.3. Synthesis of hexagonally-packed mesoporous silica (HMS) [25]

In a typical preparation, tetraethyl orthosilicate (1.0 mol) was added with vigorous stirring to a solution of dodecylamine (DDA) (0.27 mol) (in 4:1 molar ratio of tetraethyl orthosilicate to DDA) in ethanol (9.09 mol). The reaction mixture was aged at ambient temperature for 18 h, and the resulting mesoporous silica was air dried on a glass plate. The template was removed by mixing 1 g of the air-dried HMS with 150 ml of hot ethanol for 1 h. The prod-

uct was then filtered and washed with a second 100 ml portion of ethanol. This extraction procedure was repeated twice, and the crystalline product air-dried at 80 °C. Another three batches of HMS silica were prepared according to the procedure below, but using different molar ratios of tetraethyl orthosilicate to dodecyl-amine (3:1, 2:1, and 1:0.75). Also C_6-HMS, C_8-HMS and C_{10}-HMS were prepared as per the same procedure, but employing hexyl-amine, octylamine and decylamine template, respectively.

4.4. Synthesis of Ti grafted mesoporous silicas

0.2 equiv. of tetrabenzyl titanium (or tribenzyl titanium), as cal-culated on the basis of 33% Si in the porous oxide was added to a suspension of HMS mesoporous silica in dry toluene under nitro-gen. After 1 day of stirring to ensure complete absorption of the organometallic, the reduced material was collected by suction fil-tration under nitrogen and washed several times with toluene. In the case of tetrabenzyl titanium only, the reduced material was activated by heating at 120 °C for 6 h under vacuum at 10^{-3} Torr on a Schlenk line until all volatiles had been removed. This mate-rial was used as either a powder or a 1.3 cm diameter pellet com-pressed in a commercial pellet press at 4 metric tones. Assuming 1 g of $0.2TiBz_4$-HMS, with a surface area of 1165 m^2/g (1.165×10^{21} nm^2) and 4.12 wt.% Ti for $0.2TiBz_4$-HMS by elemental analysis, 1 g of $0.2TiBz_4$-HMS contains 41.2 mg Ti (8.60×10^{-4} moles Ti). The Ti coverage can then be calculated as follows: Ti coverage = (8.60×10^{-4} moles Ti $\times 6.02 \times 10^{23}$ Ti/mole)/(1.16×10^{21} nm^2)=0.4443 Ti/nm^2.

4.5. Synthesis of trimethyl Ti grafted silica [26]

$TiMe_3$ was prepared by adding $TiCl_3 \cdot 3THF$ in THF to $MeMgCl$ in THF at −40 °C drop wise over 3 h, followed by stirring for another 3 h. A deep green solution was obtained. The $TiMe_3$ solution was treated immediately with mesoporous silica placed into a side adaptor connected to the 3-neck flask reaction compartment. The temperature was then allowed to warm to ambient over several hours followed by further stirring at room temperature for 4 h. At this stage the solution was colorless and the silica had taken on a green color, suggesting complete absorption of the Ti. The solution was then filtered under inert atmosphere in the glove box and washed 3 times with THF in order to purge the sample of $MgCl_2$. The solid was then dried *in vacuo* and stored under nitro-gen before use.

4.6. Synthesis of (Allyl)₃Ti grafted silica [27,28]

The preparation procedure for $Allyl_3Ti$ was similar to that of $TiMe_3$, but $AllylMgCl$ was used instead of $MeMgCl$. Complete absorption of the Ti was confirmed by the colorless solution after filtration and isolation of the blue-gray solid.

4.7. Measurements

Nitrogen adsorption and desorption data were collected on a Micromeritics ASAP 2010. Hydrogen uptake was measured with a commercial pressure-composition isotherm (PCI) unit provided by Advanced Materials. Highly purified hydrogen (99.9995% pur-ity) was used as the adsorbent. Before all measurements, the mate-rials were activated *in vacuo* at 573 K in order to remove any physisorbed water or volatile impurities. Leak testing, performed by running a standard AX-21 sample and by bubbles, was done prior to and during each adsorption measurement experiment. In the H_2 adsorption–desorption experiments complete reversibility was observed for all samples across the whole range of pressures.

Samples were run at liquid nitrogen temperature (77 K) and liquid argon temperature (87 K) to 60 atm.

The skeletal density was measured using a Quantachrome Ul-tra-pycnometer. When the skeletal density is used for the hydro-gen uptake measurement, the compressed hydrogen within the pores is treated as part of the sample chamber volume. Therefore, only the hydrogen physisorbed to the walls of the structure is re-corded by the PCI instrument as the adsorption capacity of the material. Thus, when H_2 adsorption is measured, the skeletal den-sity of the porous materials derived from the pycnometer is em-ployed to determine the adsorbed amount of hydrogen. However, when the total storage is measured, a value that is dependent on the compression level of the solid that contains both the hydrogen physisorbed to the walls of the pores and the hydrogen existing in the pores as a second phase, the total desktop density is used in-stead of the skeletal density. This apparent density ignores the presence of pores inside the material, and therefore the void space inside the material is not subtracted out in the measurement.

Taking both the 77 and 87 K hydrogen adsorption data, enthal-pies of adsorption were calculated using a variant of the Clausius–Clapeyron equation [22]:

$$\ln\left(\frac{P_1}{P_2}\right) = \Delta H_{ads} \frac{T_2 - T_1}{RT_1T_2} \tag{1}$$

where P_n is the pressure for isotherm n, T_n is the temperature for the isotherm n, and R is the gas constant.

Pressure as a function of the amount adsorbed was determined by using exponential fit for each isotherm; the first 10 points of the isotherms were picked up and fit to the exponential equation. This exponential equation gives an accurate fit over the pressure up to 10 atm with the goodness of fit (R^2) above 0.99. The corresponding P_1 and P_2 values at a certain amount of H_2 adsorbed at both tem-peratures can be obtained by the simulated exponential equation. Inputting these numbers into Eq. (1), we then calculate the enthal-pies of the adsorption.

Acknowledgments

References

[1] L. Schlapbach, A. Züttel, Nature 414 (2001) 353–358.
[2] http://www.hydrogen.energy.gov/annual_review06_plenary.html.
[3] V.A. Yartys, I.R. Harris, V.V. Panasyuk, Mater. Sci. 37 (2001) 219.
[4] J.L.C. Rowsell, A.R. Milward, K.S. Park, O.M. Yaghi, J. Am. Chem. Soc. 126 (2004) 5666.
[5] M. Dinca, J.R. Long, Angew. Chem., Int. Ed. 47 (2008) 6766–6779.
[6] J.G. Vitillo, L. Regli, S. Chavan, G. Ricchiardi, G. Spoto, P.D.C. Dietzel, S. Bordiga, A. Zecchina, J. Am. Chem. Soc. 130 (2008) 8386–8396.
[7] A.C. Dillon et al., Nature 386 (1997) 377.
[8] Y. Ye et al., Appl. Phys. Lett. 74 (1999) 2307.
[9] T. Yildirim, S. Ciraci, Phys. Rev. Lett. 94 (2005) 175501.
[10] S.K. Bhatia, A.L. Myers, Langmuir 22 (2006) 1688.
[11] Y. Zhao, Y. Kim, A.C. Dillon, M.J. Heben, S.B. Zhang, Phys. Rev. Lett. 94 (2005) 155504.
[12] G.J. Kubas, R.R. Ryan, B.I. Swanson, P.I. Vergamini, H.J. Wasserman, J. Am. Chem. Soc. 108 (1984) 7000.
[13] G.J. Kubas, Chem. Rev. 107 (10) (2007) 4152–4205.
[14] S.S. Kaye, J.R. Long, J. Am. Chem. Soc. 127 (2005) 6506.
[15] A. Hamaed, M. Trudeau, D.M. Antonelli, J. Am. Chem. Soc. 130 (22) (2008) 6992–6999.
[16] X. Hu, M. Trudeau, D.M. Antonelli, Chem. Mater. 19 (2007) 1388.
[17] X. Hu, B. Skadtchenko, M. Trudeau, D.M. Antonelli, J. Am. Chem. Soc. 128 (2006) 11740.
[18] L.T. Zhuravlev, Colloid Surf. A Physicochem. Eng. Aspect 173 (2000) 1–38.
[19] J. Mathias, G. Wannemacher, J. Colloid. Interf. Sci. 125 (1988) 61.
[20] G.A. Nesterov, V.A. Zakharov, E.A. Paukshtis, E.N. Yurchenko, Y.I. Ermakov, Kinetika I Kataliz 20 (1979) 429–436.

[21] F. Langerame, A.M. Salvi, M. Silletti, G. Moretti, Surf. Interf. Anal. 40 (2008) 695–699.
[22] F. Roquerol, J. Roquerol, K. Sing, Adsorption by Powders and Solids: Principles, Methodology, and Applications, Academic Press, London, 1999.
[23] U. Zuchni, E. Albizatti, U. Gianni, J. Organomet. Chem. 26 (1971) 377.
[24] N.G. Maksimov, G.A. Nesterov, V.A. Zakharov, P.V. Stchastnev, V.F. Anufrienko, Y.I. Yermakov, J. Mol. Catal. 4 (1978) 167.
[25] P.T. Tanev, T.J. Pinnavaia, Science 267 (1995) 865.
[26] W. Shafer, K.H. Thiele, Z. Anorg. Allg. Chem. 447 (1978) 136.
[27] O.N. Yakovleva, O.K. Sharev, K.G. Miesserov, T.K. Vydrina, G.N. Bondarenko, E.I. Tinyakova, B.A. Dolgoplosk, Dokl. Akad. Nauk. SSSR 218 (1974) 593.
[28] S.I. Beilin, I.N. Markevich, S.B. Gol'shitein, G.N. Bondarenko, B.A. Dolgoplosk, Dokl. Akad. Nauk. SSSR 218 (1974) 837.